The Nature of the LUMO in $Fe_2(CO)_6S_2$ and the Bonding in $Fe_2(CO)_6S_2^{2-}$

Roger L. DeKock,[*1] Evert Jan Baerends, and Rudy Hengelmolen

*Department of Inorganic and Theoretical Chemistry, Free University, De Boelelaan 1083,
1081 HV Amsterdam, The Netherlands*

Received August 3, 1983

Hartree–Fock–Slater calculations are reported for $Fe_2(CO)_6S_2^n$ ($n = 0, 2-$) and for $Fe_2(CO)_6(PH_2)_2$. Analysis of the lowest unoccupied molecular orbital (LUMO) of $Fe_2(CO)_6S_2$ shows that it is S–S antibonding in contrast to the situation for $Fe_2(CO)_6(PH_2)_2$ and $Co_2(CO)_6C_2H_2$ for which the LUMO is metal–metal antibonding. Whereas the upper occupied MOs of $Fe_2(CO)_6S_2$ are mainly metal in character, those of the dianion are predominantly sulfur. The S–S bond is predicted to be significantly lengthened in the dianion as a result of large involvement of the σ_u orbital of S_2 in the cluster molecule. This work shows that molecules with similar electron counts [$Fe_2(CO)_6S_2$–$Co_2(CO)_6C_2H_2$ and $Fe_2(CO)_6S_2^{2-}$–$Fe_2(CO)_6(PH_2)_2$] can have decidedly different frontier electronic structure.

## Introduction

The geometrical structures and chemical bonding of the ligand-bridged $Fe_2(CO)_6X_2$ type dimers containing metal–metal interactions have been of interest for some time. For X_2 denoting the disulfur ligand S_2, Wei and Dahl[2] reported the X-ray structure in 1965. For X_2 denoting the $(PR_2)_2$ ligand (R = phenyl) the X-ray structure was determined in Dahl's laboratories and reported in Ph.D. thesis form in 1973.[3] More recently, Dahl and co-workers have reported the crystal structure of the dianion of the latter compound.[4]

Coupled with this crystallography work has been a study of the electronic structure and chemical bonding of these types of compounds. The initial work in this area was carried out by Teo, Hall, Fenske, and Dahl.[5] Regarding the neutral compounds mentioned here, it was concluded that "the orbital character of the a_1 HOMO in each neutral species is found to correspond closely to the classical "bent" Fe–Fe bond with the b_2 LUMO being its antibonding counterpart". Subsequent to this landmark paper, extended Hückel and self-consistent field Xα–scattered wave (SCF Xα–SW) calculations have been reported by Andersen et al.,[6] as part of a larger study reporting the ultraviolet photoelectron spectrum of $Fe_2(CO)_6S_2$. Similar experimental and theoretical studies also were carried out by Van Dam et al.,[7] utilizing the ab initio method in their theoretical studies. The latter authors also studied $Co_2(CO)_6C_2H_2$,[8] which has the same number of valence electrons as $Fe_2(CO)_6S_2$. More recently, we have reported on the results of our Hartree–Fock–Slater (HFS) calculations on $Fe_2(CO)_6S_2$ with a view to examining the nature of the Fe–Fe bonding in the molecule.[9]

In addition to these theoretical studies, the crystal structure of $Fe_2(CO)_6(PPh_2)_2^{2-}$ is most easily understood by assuming that the Fe–Fe antibonding MO is occupied by two electrons in going from the neutral to the dianion.[4]

With this background in mind, and the initial reports of Seyferth et al.[10] on the chemistry of the dianion $Fe_2(CO)_6S_2^{2-}$, it was no wonder that the first question after the plenary lecture of Seyferth at the 181st American Chemical Society Meeting[11] dealt with the nature of the LUMO for $Fe_2(CO)_6S_2$. That is, if the LUMO is Fe–Fe antibonding, why should $Fe_2(CO)_6S_2^{2-}$ be represented as in 1, indicating implicitly that the additional two electrons

1
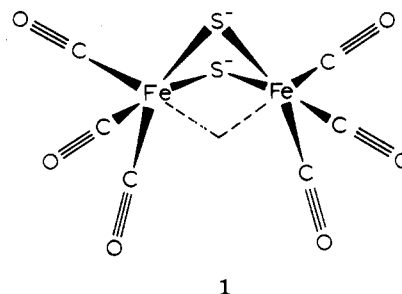
have occupied an orbital that is mainly S–S antibonding rather than Fe–Fe antibonding? At the time this question remained unanswered. Such is the background to this communication.

The Calculations

The calculations reported in this work were carried out by utilizing the HFS method developed in these laboratories.[12] The basis set was double ζ; the only polarization functions were the 4p orbitals on Fe that were single ζ (Slater exponent 2.0). Numerous studies employing the HFS method have shown it to provide excellent results in comparison to a wide variety of experimental probes.[13] In

(1) Correspondence to: Department of Chemistry, Calvin College, Grand Rapids, MI 49506.

(2) Wei, C. H.; Dahl, L. F. *Inorg. Chem.* 1965, *4*, 1.

(3) Huntsman, J. R. Ph.D. Thesis, University of Wisconsin—Madison, 1973.

(4) Ginsburg, R. E.; Rothrock, R. K.; Finke, R. G.; Collman, J. P. Dahl, L. F. *J. Am. Chem. Soc.* 1979, *101*, 6550.

(5) Teo, B. K.; Hall, M. B.; Fenske, R. F.; Dahl, L. F. *Inorg. Chem.* 1975, *14*, 3103.

(6) Andersen, E. L.; Fehlner, T. P. Foti, A. E.; Salahub, D. R. *J. Am. Chem. Soc.* 1980, *102*, 7422. Andersen's name was misspelled in the heading of this reference. The correct spelling is employed here.

(7) Van Dam, H.; Louwen, J. N.; Oskam, A.; Doran, N.; Hillier, I. H. *J. Electron Spectrosc. Relat. Phenom.* 1980, *21*, 57. This reference employs a b_1,b_2 notation the opposite of that used in this work and the other references.[5,6]

(8) Van Dam, H.; Stufkens, D. J.; Oskam, A.; Doran, M.; Hillier, I. H. *J. Electron Spectrosc. Relat. Phenom.* 1980, *21*, 47.

(9) DeKock, R. L.; Baerends, E. J.; Oskam, A. *Inorg. Chem.* 1983, *22*, 4158.

(10) Seyferth, D.; Henderson, R. S.; Song, L. *J. Organomet. Chem.* 1980, *192*, C1. Seyferth, D.; Henderson, R. S.; Song, L. *Organometallics* 1982, *1*, 125.

(11) Seyferth, D. "Abstracts of Papers", 181st National Meeting of the American Chemical Society, Atlanta, GA 1981; American Chemical Society: Washington, DC, 1981.

(12) Baerends, E. J.; Ros, P. *Int. J. Quantum Chem.* 1978, *12S*, 169. Heijser, W.; Baerends, E. J.; Ros, P. *Faraday Discuss. Chem. Soc.* 1980, *No. 14*, 211.

(13) Ellis, D. E.; Baerends, E. J.; Adachi, H.; Averill, F. W. *Surf. Sci.* 1977, *64*, 649. Rosén, A.; Baerends, E. J.; Ellis, D. E. *Ibid.* 1979, *82*, 139. Ziegler, T.; Snijders, J. G.; Baerends, E. J. *J. Chem. Phys.* 1981, *74*, 1271. Famiglietti, C.; Baerends, E. J. *Chem. Phys.* 1981, *62*, 407. Post, D.; Baerends, E. J. *J. Chem. Phys.* 1983, *78*, 5663.
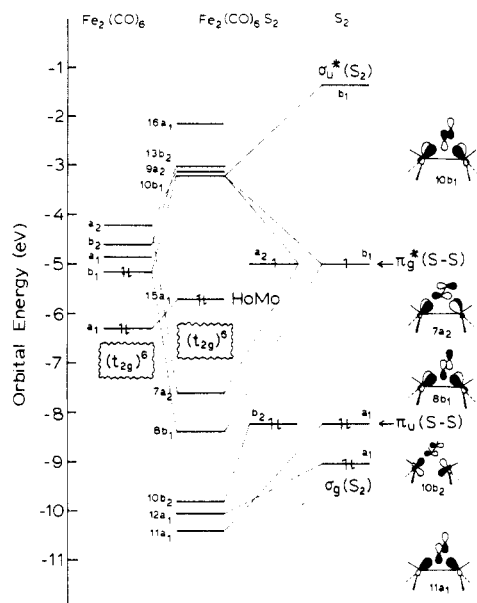
Figure 1. Energy level diagram for $Fe_2(CO)_6S_2$. Only major correlation lines are drawn. For example, $16a_1$ correlates with the empty a_1 orbital of $Fe_2(CO)_6$; $11a_1$ $12a_1$, and $10b_2$ correlate also with frontier orbitals of $Fe_2(CO)_6$. The relatively nonbonding set labeled $(t_{2g})^6$ spans a_1, a_1, a_2, b_1, b_2, and b_2.

addition to providing useful information on molecular ground states, the HFS method is known to be capable of accurately describing excited-state properties of molecules, such as UV–visible spectra.[14] The relative energies of occupied and virtual molecular orbitals is usually maintained upon going from the ground state to calculations involving a separate transition-state calculation for each excited state. Hence, we feel that the HFS method is thoroughly suited to undertake the type of question being posed in this paper. A word of caution is always in order for any study concerned with empty (virtual) orbitals. In our case, we are able to monitor the change in the LUMO of $Fe_2(CO)_6S_2$ upon going to the dianion; this provides a degree of trustworthiness to the conclusions.

We employed geometries based upon the experimental structures quoted above, with appropriate averaging of bond angles and bond lengths to maintain C_{2v} symmetry for each molecule or ion. In all cases we retained the same basic $Fe_2(CO)_6$ structure that has been reported for the $Fe_2(CO)_6S_2$ molecule.[2] The S–S distance in the neutral compound was set at the experimental value of 2.0 Å, whereas the dianion calculation was done both at 2.0 and at 2.9 Å. The latter value is an estimate based upon the S–S distance in compounds containing substituents on the S atoms such as $Fe_2(CO)_6(SCH_3)_2$.[15] The P–P distance in the phosphorus compound also was set at 2.9 Å, in accord with known structural results on such compounds.[3,4] A P–H distance of 1.44 Å was employed, and the hydrogen positions were chosen on the basis of the positions of heavier substituents as determined in the crystallographic studies.[3,4]

Results and Discussion

A. Observations Regarding the LUMO of $Fe_2(CO)_6S_2$. The basic bonding of a bridged cluster such as $Fe_2(CO)_6S_2$ is well understood. The gist of the frontier orbitals involving the Fe_2S_2 cluster is presented in Figure

(14) Ziegler, T.; Rauk, A.; Baerends, E. J. *Chem. Phys.* **1976**, *16*, 209. Trsic, M.; Laidlaw, W. G.; Oakley, R. T. *Can. J. Chem.* **1982**, *60*, 2281.
(15) Dahl, L. F.; Wei, C. H. *Inorg. Chem.* **1963**, *2*, 328.

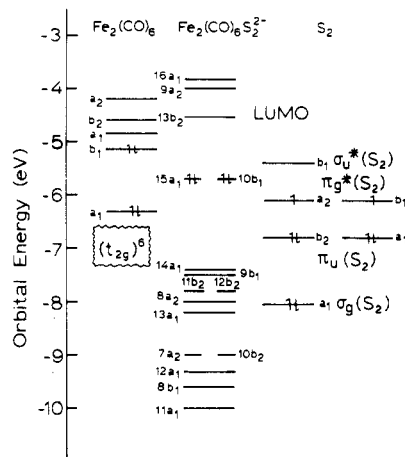**Figure 2.** Energy level diagram for $Fe_2(CO)_6S_2^{2-}$. A scale shift of +10 eV has arbitrarily been added to the eigenvalues of the dianion to place its eigenvalues on the same scale as that for the neutral fragments. An S–S bond length of 2.9 Å was used.

1, as derived from our HFS results on $Fe_2(CO)_6S_2$. Not presented are the 60 electrons mainly involved in the CO ligands or the four electrons of S_2 derived from $\sigma_g(3s)$ and $\sigma_u(3s)$.

Bonding of S_2 to the $Fe_2(CO)_6$ substrate is due to stabilization of the occupied $\pi_u(a_1)$ and $\pi_u(b_2)$ orbitals of S_2 by appropriate frontier orbitals of $Fe_2(CO)_6$ and by mixing of the half-occupied $\pi_g^*(b_1)$ and $\pi_g^*(a_2)$ with frontier orbitals of $Fe_2(CO)_6$. There results a set of *three* MOs clustered together in the virtual spectrum: π_g^*-$Fe_2(CO)_6$ antibonding orbitals $9a_2$ and $10b_1$ (also S–S antibonding) and a π_u-$Fe_2(CO)_6$ antibonding orbital, $13b_2$ (mainly the Fe–Fe antibonding counterpart of the $15a_1$ HOMO, the bent Fe–Fe bond).

These results for the virtual orbitals are quite different from those presented in the previous calculations, in which the b_2 Fe–Fe antibonding orbital was the LUMO and resided with a gap of 0.6^6 to 2.8 eV[16] between itself and the other two virtual orbitals (a_2 and b_1). The implications of this result on the structure and bonding of the dianion $Fe_2(CO)_6S_2^{2-}$ are quite dramatic. We have carried out numerous calculations on the dianion and on $Fe_2(CO)_6(PH_2)_2$ to examine these implications.

1. Calculations on the dianion with the geometry of the neutral molecule indicate a slight preference (16 kcal/mol) for occupation of the $10b_1$ S–S antibonding orbital, using the Ziegler transition-state method for energy analysis.[17] This energy preference is similar to the difference in energy between the two eigenvalues ($10b_1$ and $13b_2$) in the ground-state calculation (6 kcal/mol). However, the HOMO–LUMO gap is only a few kilocalories per mole for the dianion with the neutral molecule geometry so that this configuration is expected to be very unstable.

2. Calculations on the dianion with a lengthened S–S bond (to 2.9 Å) show a dramatic stabilization of the $10b_1$ S–S antibonding orbital (Figure 2). The eigenvalue has now stabilized by 56 kcal/mol compared to the value for the shorter S–S bond length, and the total energy has stabilized by 80 kcal/mol. Occupation of the $10b_1$ MO should result in a stable species.

(16) This value of 2.8 eV was not reported in ref 5; we have independently carried out Fenske–Hall calculations on $Fe_2(CO)_6S_2$ to check this point.
(17) Ziegler, T.; Rauk, A. *Theor. Chim. Acta* **1977**, *46*, 1. Ziegler, T.; Rauk, A. *Inorg. Chem.* **1979**, *18*, 1558, 1755. Baerends, E. J.; Post, D. In "Quantum Theory of Chemical Reactions"; Daudel, R., Pullman, A., Salem, L., Veillard, A., Eds.; D. Reidel Publishing Co.: Dordrecht, The Netherlands, 1982; Vol. III, p 15.

Table I. Mulliken Overlap Populations and Atomic Charges

species	total[a] (Fe-S)	total (S-S)	b₁ (Fe-S)[b]	b₁ (S-S)[b]	Q_{Fe}	Q_S
$Fe_2(CO)_6S_2$	0.244	0.020	0.035	-0.264	-0.26	+0.13
$Fe_2(CO)_6S_2^{2-}$ (S-S = 2.0 Å)	0.135	-0.642	-0.073	-0.832	-0.22	-0.19
$Fe_2(CO)_6S_2^{2-}$ (S-S = 2.9 Å)	0.287	-0.251	0.019	-0.586	-0.22	-0.25

[a] Per Fe-S bond. [b] For MOs 8b₁, 9b₁, and 10b₁. The latter is empty for the neutral complex.

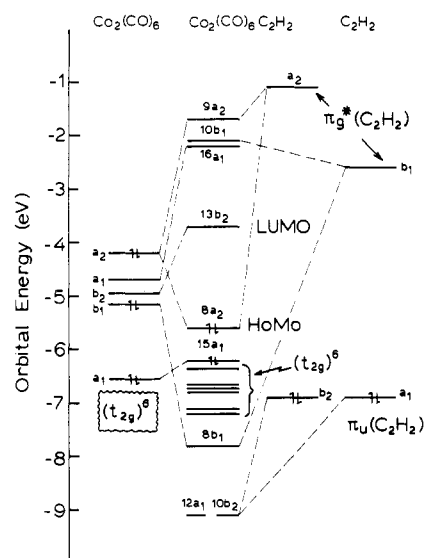**Figure 3.** Energy level diagram for $Co_2(CO)_6C_2H_2$. The portion of the diagram referring to C_2H_2 is for the perturbed ligand with $r(C-C) = 1.34$ Å and angle CCH = 145°. This accounts for the nondegeneracy of the π^* (a₂ and b₁) levels.

3. Our findings for $Fe_2(CO)_6S_2^{2-}$ are in accordance with the results we obtained on $Fe_2(CO)_6(PH_2)_2$, isoelectronic with the dianion. The LUMO of these two species is the 13b₂ Fe-Fe antibonding MO, as implicated in the crystallographic study of $Fe_2(CO)_6(PPh_2)_2^{2-}$.[4] In the case of the PH_2-derived cluster, the counterpart of 10b₁ for the sulfur dianion cluster is stabilized below the mainly Fe 3d MOs because the protons lower the energy of this orbital substantially.[18]

4. Finally, we have made a comparison of our $Fe_2(CO)_6S_2$ energy level diagram with that of $Co_2(CO)_6C_2H_2$ (Figure 3); both molecules have the same number of valence electrons. Notice that in this case the LUMO is clearly the 13b₂ Co-Co antibonding MO. This calculated character of the LUMO is consistent with the electron spin resonance results for $Co_2(CO)_6C_2H_2^-$.[19] The change in character of the LUMO for $Co_2(CO)_6C_2H_2$ compared to $Fe_2(CO)_6S_2$ is understandable in terms of hypothetical proton shifts from the Co atoms and the H atom positions to the C atoms to transform the C atoms into O(S) atoms. Such a transferral would certainly stabilize the π^* MOs of the ligand S_2 compared to C_2H_2, as observed in our calculations. It is this stabilization that lowers the energy of 10b₁ for $Fe_2(CO)_6S_2$ so that it becomes the LUMO, rather than 13b₂.

We also have carried out calculations on the hypothetical ion $Fe_2(CO)_6P_2^{2-}$, and the relative shifts in energy levels compared to $Fe_2(CO)_6S_2$ provide additional support for the effect of proton transferral on the virtual MOs as described

above. That is, the P_2 ligand, with two protons less than S_2, exhibits a destabilized π_g^* set of orbitals so that 13b₂ is the LUMO, and 10b₁ (derived from π_g^*) is destabilized.

B. Electronic Structure of $Fe_2(CO)_6S_2^{2-}$ Compared to $Fe_2(CO)_6S_2$. The electronic structure and bonding of $Fe_2(CO)_6S_2$ is well understood and has been adequately commented upon previously.[5-7,9] The orbital energy level diagram already has been presented in Figure 1; the four major $S_2-Fe_2(CO)_6$ interaction orbitals are also depicted in Figure 1. At higher energy than the four interaction orbitals are the "$(t_{2g})^6$"-derived nest of Fe-Fe "nonbonding" MOs, followed by the HOMO which is typically described as the Fe-Fe "bent" bond.

As can be seen by comparing Figures 1 and 2, the orbital energy level diagram for $Fe_2(CO)_6S_2^{2-}$ is quite different from that for $Fe_2(CO)_6S_2$. In order to analyze the difference in bonding between these two species, we shall begin by considering the consequences of adding two electrons to the cluster molecule while maintaining the same geometry. The orbital energy pattern and nature of the MOs remain essentially unchanged upon adding the two electrons to the 10b₁ orbital. This results in a very unstable situation for two reasons. First, there is now a very small HOMO-LUMO gap since the 9a₂ and 13b₂ levels lie very close to the 10b₁ level. Second, the 10b₁ level is both Fe-S and S-S antibonding as depicted in Figure 1.

Pertinent Mulliken overlap populations and atomic charges are presented in Table I. In addition to total overlap populations we present also the overlap populations associated with the 8b₁, 9b₁, and 10b₁ MOs since these MOs undergo the most significant changes in the subsequent analysis. Notice that the trend in total overlap population is mirrored by that in these three b₁ orbitals. Close examination of the atomic charges on the Fe and S atoms reveals that of the two electrons added to the molecule, only 0.56 additional electrons reside on the four atoms in the cluster. In other words the Fe atoms function as effective electron "transmitters" and the CO ligands as effective electron "sinks" even in this unstable dianion configuration. Nevertheless, the 10b₁ orbital is sufficiently antibonding to cause the Fe-S and S-S overlap populations to decrease substantially. The nature of the Fe-S antibonding interaction is depicted in Figure 1 and results from mixing of the $Fe_2(CO)_6$ HOMO (b₁) with the π_g^* orbital of S_2. The large negative S-S overlap population is a result not only of the 36% character of π_g^* in this orbital but also of the 14% of σ_u^*. The latter orbital is much more antibonding than the π_g^* orbital as seen by comparing the Mulliken overlap populations for the two orbitals based upon one electron occupancies: -2.34 vs. -0.31. There is little overlap between the b₁ HOMO of $Fe_2(CO)_6$ and σ_u^* of S_2 since the metal orbitals have their maximum projection toward the nodal regions of the S 3p orbitals in σ_u^*. This small interaction turns into a bonding interaction upon lengthening of the S-S bond (Figure 4).

We now turn to an examination of the effects of lengthening the S-S bond upon the net bonding in the cluster molecule. As can be seen by comparing the S_2 portion of the energy level diagrams in Figures 1 and 2, S-S bond lengthening results in bringing the 3p-derived S_2 eigenvalues closer together in energy. The most dra-

---

(18) As a footnote, we observe that the ground-state electronic structure and orbital character of the upper occupied (mainly 3d) MOs of $Fe_2(CO)_6(PH_2)_2$ are very similar to those of $Fe_2(CO)_6S_2$. This observation is in agreement with that of Teo et al.,[5] and essentially is due to the fact that the "stretched" P_2H_4 ligand (P-P = 2.9 Å) presents a set of frontier orbitals to $Fe_2(CO)_6$ not unlike that of S_2 at S-S = 2.0 Å.

(19) Peake, B. M.; Rieger, P. H.; Robinson, B. H.; Simpson, J. *J. Am. Chem. Soc.* **1980**, *102*, 156.

view along Fe–Fe axis
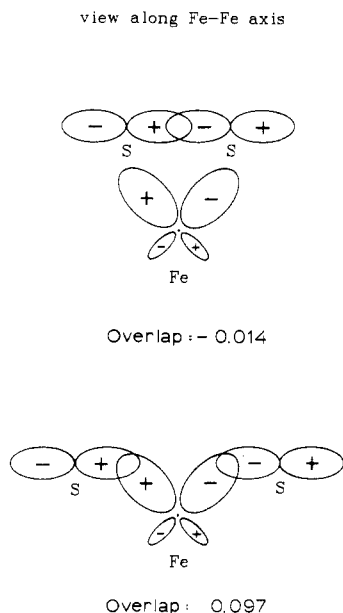

Overlap : – 0.014

Overlap : 0.097

Figure 4. Overlap between the $\sigma_u{}^*$ S_2 orbital and the b_1 HOMO of $Fe_2(CO)_6$ for S–S bond lengths of 2.0 and 2.9 Å. We view along the y direction. The Fe–Fe bond is the y axis. The d orbitals are d_δ with respect to the Fe–Fe bond. Each Fe d_δ orbital has the sign of the one depicted. The small negative overlap at the shorter S–S bond length turns into a sizeable positive overlap at the longer S–S bond length.

matic effect is the lowering of the $\sigma_u{}^*$ orbital. The S–S σ_g and σ_u now become energetically available to participate in the cluster bonding. In addition, the $\pi_g{}^*$ and $\pi_u{}^*$ orbitals of S_2 are more accessible energetically to the plethora of low-lying occupied and unoccupied orbitals of $Fe_2(CO)_6$, particularly to the $(t_{2g})^6$-derived set of six "nonbonding" MOs.

Pertinent overlap populations and charges for the resultant dianion with a stretched S–S bond also are presented in Table I. Lengthening the S–S bond both strengthens the Fe–S bond and reduces the S–S antibonding effect. Meanwhile the atomic charges on the Fe and S atoms change very little.

What is not revealed by the overlap populations and charges in Table I is the extent by which the nature of the upper occupied MOs change upon going from the neutral compound with S–S at 2.0 Å to the dianion with S–S at 2.9 Å. In Table II we present the major sulfur character of these upper MOs along with the Fe–S overlap population for each MO. Notice that for $Fe_2(CO)_6S_2$ the S_2–$Fe_2(CO)_6$ interaction MOs ($11a_1$, $7a_2$, $8b_1$, and $10b_2$) contain significant S character and that these four MOs also have the largest Fe–S overlap population. Of most interest for the dianion is that the major sulfur character is now distributed over 11 MOs instead of only four interaction MOs. This is a result of the sulfur AOs mixing with the "$(t_{2g})^6$" MOs of $Fe_2(CO)_6$ so that such a nest of mainly nonbonding 3d MOs no longer exists (compare Figures 1 and 2). For our purposes the most significant change in MO character occurred for the $15a_1$ and $10b_1$ MOs, the two most high-lying orbitals in the dianion. The $15a_1$ MO has changed from being mainly the "bent" Fe–Fe bond in the neutral molecule to an Fe–S antibond that is mainly sulfur in the dianion. In the neutral molecule the $10b_1$ MO was mainly (Fe–S)* and (S–S)* and unoccupied whereas in the dianion it is mainly $\sigma_u{}^*$ (55%) and $\pi_g{}^*$ (31%) and fully occupied with two electrons.

The consequences of this changed orbital character are twofold. On the theoretical side the significantly length-

Table II. Iron–Sulfur Overlap Populations and Major Sulfur Character for the Upper Occupied MOs of $Fe_2(CO)_6S_2$ and $Fe_2(CO)_6S_2{}^{2-}$ (S–S = 2.9 Å)

orbital	$Fe_2(CO)_6S_2$		$Fe_2(CO)_6S_2{}^{2-}$	
	(Fe–S)[a]	S character	(Fe–S)[a]	S character
11a₁	0.059	36% π_u, 33% σ_g	0.071	46% σ_g
12a₁	0.026	53% σ_g	0.048	29% π_u
13a₁	–0.040	8% σ_g	0.007	
14a₁	–0.015	8% π_u	–0.037	31% σ_g
15a₁	–0.022		–0.102	48% π_u, 7% σ_g
7a₂	0.067	62% π_g	0.079	53% π_g
8a₂	0.001		0.001	
9a₂	–0.102[b]	34% π_g	–0.106[b]	42% π_g
8b₁	0.046	43% π_g	0.028	22% π_g, 10% σ_u
9b₁	–0.011	17% π_g	–0.012	14% π_g, 8% σ_u
10b₁	–0.107[b]	36% π_g, 14% σ_u	0.003	31% π_g, 55% σ_u
10b₂	0.056	61% π_u	0.061	31% π_u
11b₂	0.001		0.024	16% π_u
12b₂	0.001		–0.007	18% π_u
13b₂	–0.067[b]	10% π_u	–0.039[b]	18% π_u

[a] The overlap populations are per Fe–S bond. [b] These orbitals are empty, but the overlap population has been calculated as though there were two electrons in the orbital.

ened S–S bond is now understood as being due to the large amount of $\sigma_u{}^*$ character in the $10b_1$ MO of the dianion. In other words we cannot view $Fe_2(CO)_6S_2{}^{2-}$ as being composed of $Fe_2(CO)_6$ and $S_2{}^{2-}$, since the latter would be expected to have an S–S bond length only slightly longer than 2.0 Å.[20] Consequently, we can say that the S–S bond has been lengthened or "activated" by about 0.9 Å as a result of the participation of the $\sigma_u{}^*$ orbital in the bonding of the dianion. On the experimental side the changed orbital character of $15a_1$ and $10b_1$ allows us to understand why the reactivity of $Fe_2(CO)_6S_2{}^{2-}$ toward a variety of reagents is at the sulfur centers,[10] because the upper two occupied MOs are mainly sulfur in character.

Finally we comment upon the difference between Fe_2-$(CO)_6S_2{}^{2-}$ and the unknown $Co_2(CO)_6N_2{}^{2-}$. Whereas the former allows electron occupation of the $10b_1$ MO with the resultant activation of the S–S bond, the latter would allow occupation of the $13b_2$ MO which is mainly Co–Co antibonding just as for isoelectronic $Co_2(CO)_6C_2H_2$ (compare Figures 1 and 3). Therefore reduction of the cobalt nitrogen complex (if prepared) would not be a good candidate to explore activation of the N_2 molecule.[22]

(20) We expect little bond length change between S_2 and $S_2{}^{2-}$ for the following reason: there are large bond length differences for first-row diatomics such as N_2, O_2, and F_2 or O_2, $O_2{}^-$, and $O_2{}^{2-}$, but only slight bond length changes in the series P_2, S_2, and Cl_2 (see ref 21). For a discussion of S–S bond lengths see ref 5.

(21) DeKock, R. L.; Gray, H. B. "Chemical Structure and Bonding"; Benjamin/Cummings Publishing Co.: Menlo Park, CA, 1980.

(22) For extended Hückel calculations on $Co_2(CO)_6N_2$ see: Goldberg, I.; Hoffman, D. M.; Hoffmann, R. *Inorg. Chem.* **1982**, *21*, 3863.